



Top-down and bottom-up estimates of anthropogenic methyl bromide emissions from eastern China

Haklim Choi¹, Mi-Kyung Park¹, Paul J. Fraser², Hyeri Park³, Sohyeon Geum³, Jens Mühle⁴, Jooil Kim⁴, Ian Porter⁵, Peter K. Salameh⁴, Christina M. Harth⁴, Bronwyn L. Dunse², Paul B. Krummel²,
5 Ray F. Weiss⁴, Simon O'Doherty⁶, Dickon Young⁶, and Sunyoung Park^{1,3}

¹Kyungpook Institute of Oceanography, Kyungpook National University, Daegu 41566, Republic of Korea

²Climate Science Centre, Commonwealth Scientific and Industrial Research Organisation (CSIRO) Oceans and Atmosphere, Aspendale, Victoria 3195, Australia

10 ³Department of Oceanography, Kyungpook National University, Daegu 41566, Republic of Korea

⁴Scripps Institution of Oceanography, University of California San Diego, La Jolla, California 92093, USA

⁵School of Life Sciences, La Trobe University, Bundoora, Victoria 3086, Australia

⁶Atmospheric Chemistry Research Group, University of Bristol, Bristol BS8 1TS, UK

15

Correspondence to: Sunyoung Park (sparky@knu.ac.kr)

Abstract. Methyl bromide (CH₃Br) is a potent ozone-depleting substance (ODS) that has both natural and anthropogenic sources. CH₃Br has been used mainly for preplant soil fumigation, post-harvest grain and timber fumigation and structural fumigation. Most non-quarantine/pre-shipment (non-QPS) uses have been phased-out in 2005 for non-Article 5 (developed) countries and in 2015 for Article 5 (developing) countries under the Montreal Protocol on Substances that Deplete the Ozone Layer; some uses have continued under critical use exemptions (CUEs). Under the Protocol, individual nations are required to report annual data on CH₃Br production and consumption for quarantine/pre-shipment (QPS) uses, non-QPS uses and CUEs to the United Nations Environment Programme (UNEP). In this study, we analyzed high precision, *in situ* measurements of atmospheric concentrations of CH₃Br obtained at the Gosan station on Jeju island, Korea, from 2008 to 2019. The background concentrations of CH₃Br in the atmosphere at Gosan declined from 8.5 ± 0.8 ppt in 2008 to 7.4 ± 0.6 ppt in 2019 at a rate of -0.13 ± 0.02 ppt yr⁻¹. At Gosan, we also observed periods of persistent concentrations (pollution events) elevated above the decreasing background in continental air masses from China. Statistical back trajectory analyses showed that these pollution events predominantly trace back to CH₃Br emissions from eastern China. Using an inter-species correlation (ISC) method with the reference trace species CFC-11 (CCl₃F), we estimate anthropogenic CH₃Br emissions from eastern China at 4.1 ± 1.3 Gg yr⁻¹ in 2008–2019, approximately 2.9 ± 1.3 Gg yr⁻¹ higher than the bottom-up emission estimates reported to UNEP. Possible non-fumigation CH₃Br sources - rapeseed production and biomass burning – were assessed and it was found that the discrepancy is more likely due to unreported or incorrectly reported QPS and non-QPS fumigation uses. These largely-unreported anthropogenic emissions of CH₃Br are confined to eastern China and account for 30–40% of anthropogenic global

20
25
30



CH₃Br emissions. They are likely due to delays in the introduction of CH₃Br alternatives, such as sulfuryl fluoride (SO₂F₂),
35 heat, irradiation and a possible lack of industry awareness of the need for regulation of CH₃Br production and use.

1 Introduction

Methyl bromide (CH₃Br) is a colorless, odorless, non-flammable chemical that is a powerful ozone-depleting substance (ODS).
Apart from the issue of ozone layer depletion, there are the public health concerns associated with CH₃Br toxicity, for example
40 the risk of poisoning workers handling the chemical. CH₃Br has been widely used for fumigation to eradicate various pests
present in soils or in the storage, import and export of grains and timbers. CH₃Br was listed in 1992 as an ODS under the
Montreal Protocol (MP) on Substances that Deplete the Ozone Layer, an international agreement for the protection of the
stratospheric ozone layer. The Parties to the Protocol agreed to a schedule for the total phase-out of CH₃Br use, beginning with
a freeze on production and consumption in 1995 at the 1991 baseline level followed by step down reductions in 1999, 2001
45 and 2003 and total phase-out by 2005 for non-Article 5 (developed) countries and a freeze at 1995-1998 average baseline
levels and total phase out in 2015 for Article 5 (developing) countries. Typically, 91% of CH₃Br consumption for non-QPS
uses was for soil fumigation and 9% for storage products and structures in both non-Article 5 and Article 5 countries (MBTOC,
2018). Presently quarantine and pre-shipment (QPS) uses are exempt from the phase-out, however individual Parties to the
MP are required to annually report data on the CH₃Br production and consumption for QPS uses, non-QPS uses and critical
50 use exemptions (CUEs) to United Nations Environment Programme (UNEP). Except for a small use of CH₃Br for CUEs, the
consumption of CH₃Br for preplant soil fumigation and non-QPS commodities/structures has been reduced completely,
contributing to an overall reduction of over 60,000 tonnes in the global consumption of CH₃Br. The reported amounts of
consumption of CH₃Br for QPS that are not controlled (exempted from phase-out) under the MP have remained relatively
constant over the past 20 years, and now account for more than 98% of the estimated consumption of CH₃Br currently reported
55 due to the phase-out of other uses (TEAP, 2020). Despite no formal regulation, most parties to the MP are making efforts to
minimize the use of CH₃Br for QPS use and replace it with suitable alternatives such as heat treatment, phosphine (PH₃), ethyl
formate (C₂H₅OCHO), sulfuryl fluoride (SO₂F₂) and ethanedinitrile (NCCN). As a consequence of this CH₃Br phase-out, the
global atmospheric concentration of CH₃Br decreased from 9.2 ppt at the peak in 1996–1998, to 6.6 ppt in 2015, but then
showed a slight positive growth of 0.14 ppt yr⁻¹ (2.1% yr⁻¹) from 2015 to 2016 (Engel and Rigby et al., 2019).
60 Since CH₃Br has a relatively short lifetime (0.8 year) compared to the other major ODSs (Yvon and Butler et al., 1996; Hu et
al., 2012; Engel and Rigby et al., 2019), changes in surface emissions tend to be reflected quickly in changes to atmospheric
concentrations. Unlike most other ODSs, CH₃Br has both natural and anthropogenic sources. The principal natural emission
sources are the ocean (Hu et al., 2012), salt marshes (Montzka and Reimann et al., 2011), wetlands (Lee-Taylor and Holland,
2000), fungi (Lee-Taylor and Holland, 2000; Lee-Taylor et al., 2001) and plants such as mangroves or shrubs (Rhew et al.,
65 2001; Manley et al., 2007). Anthropogenic emission sources include fumigation (Carpenter and Reimann et al., 2014),



agricultural and biofuel biomass burning (Andreae and Merlet, 2001), and the rapeseed industry (Gan et al., 1998; Mead et al., 2008). CH_3Br is removed from the atmosphere by soil and ocean deposition, reactions with hydroxyl (OH), and photolysis mainly occurring in the lower stratosphere. The sources and sinks of CH_3Br in the atmosphere are not in balance, with total sinks larger than total sources by about 40 Gg yr^{-1} (Carpenter and Reimann et al., 2014). This is most likely due to insufficient
70 understanding of existing sources (Yokouchi et al., 2002; Montzka et al., 2003). Recently, possible new sources have been identified. For example, emissions of CH_3Br occur in the bread-baking process (Thornton et al., 2016) and from seaweed meadows (Weinberg et al., 2015), but their contributions were found to not have a significant impact on the global budget. The reasons for the imbalance between CH_3Br sources and sinks remain unresolved.

Global anthropogenic emissions of CH_3Br can be estimated using “bottom-up methods from consumption and production data
75 across various activities reported to UNEP annually by individual nations using activity-dependent emission factors. Significant uncertainties result from the emission factors and the speciation of CH_3Br consumption across various activities (Vaughn et al., 2018). As QPS uses of CH_3Br are generally highly emissive, consumption for these activities can be more accurately converted into emissions for this application (MBTOC, 2018).

“Top-down” estimates of global CH_3Br emissions are derived from modelling of measured atmospheric concentrations and
80 atmospheric transport processes, for example using the AGAGE 12-box model of the atmosphere, assuming an atmospheric lifetime for CH_3Br (Cunnold et al., 1994; Prinn et al., 2005; Rigby et al., 2013). Regional characteristics of CH_3Br emissions however cannot be obtained with the AGAGE 12-box or similar model, because they do not have the resolution to account for the synoptic scale of the atmospheric flow. Since the MP control of CH_3Br consumption applies at a national level, rather than globally, it is important to estimate the resultant top-down emissions at a regional to national scale (Weiss and Prinn, 2011).
85 China is the largest producer and consumer of agricultural products in the world and therefore has potentially large anthropogenic sources of CH_3Br and is an important region for understanding CH_3Br emissions in East Asia. Several studies have estimated the regional or national emissions from China based on “top-down” approaches using atmospheric observations. Blake et al. (2003) estimated the CH_3Br emissions of 2.6 Gg yr^{-1} in China (South China: 2.0 Gg yr^{-1} and North China: 0.6 Gg yr^{-1}) from aircraft observations in 2001. An inverse modeling study (Vollmer et al., 2009) using high-frequency ground
90 measurements suggested emissions from China had decreased to 0.24 Gg yr^{-1} in 2006–2008. However, those results were based on a limited period of observations (e.g., few months to years) and could not analyze the long-term variations and trends in CH_3Br emissions. Since then, there have been no further studies tracking the CH_3Br emission trends in East Asia.

In this study, we present the 12-year high-precision, high-frequency record of atmospheric CH_3Br concentrations observed at Gosan station on Jeju island, South Korea, and analyze the observed variations in atmospheric CH_3Br . We estimate annual
95 emissions of CH_3Br mainly from anthropogenic sources in eastern China, based on the empirical inter-species correlations between CH_3Br and CFC-11 during pollution episodes from eastern China and the well-defined eastern China CFC-11 emissions. This is the first study to present the long-term changes in CH_3Br emissions from eastern China, after the phase-out period. In the following sections, we first introduce (Section 2) the Gosan station and the *in situ* ground-based instrumentation for CH_3Br measurements in Section 2. In Section 3, long-term seasonal and annual variations of atmospheric CH_3Br



100 concentrations are discussed. In Sections 4 and 5, we suggest potential source regions that show high sensitivities to the enhanced CH₃Br concentrations based on air-mass back-trajectory statistics. The observation-based emission estimates of CH₃Br in eastern China are further discussed considering the existing discrepancy between the global bottom-up and top-down emissions of CH₃Br.

2 Instrumentation

105 The coastal atmospheric observation station Gosan (GSN, 33.3°N, 126.2°E, 72 m a.s.l) at the south-western tip of Jeju island, South Korea (See Figure 1) is ideally located to monitor regional background concentrations of atmospheric trace gases due to minimal influence of local anthropogenic pollution sources, and the strong pollution outflows from China, Korea, and Japan in East Asia (Kim et al.2012; Li et al., 2011 and 2014; Park et al., 2018).

The *in situ* measurement system at Gosan, a “Medusa” gas chromatography-mass spectrometer (GC-MS) equipped with a cryogenic pre-concentration system (Miller et al., 2008; Prinn et al., 2018), monitors more than 40 halogenated compounds including CFC-11 and CH₃Br. As a part of the Advanced Global Atmospheric Gases Experiment (AGAGE; Prinn et al., 2018), Gosan station has been conducting continuous high-precision and high-frequency observations approximately every 2-hours (12 times per day) from 2008 to the present. The precisions (1σ) of all species, determined from repeated analysis ($n=12$) of an ambient standard, are better than 1% (i.e., the precision of CH₃Br < 0.1%). The atmospheric abundances of most the Medusa
115 compounds are calibrated on scales maintained by the Scripps Institution of Oceanography (SIO) (e.g., SIO-05 scale for CH₃Br in this study).

3 Description of measurement data

Long-term, high-frequency CH₃Br data observed during 2008–2019 at Gosan and background concentration data from Mace Head (53.3°N, 9.9°W) and Cape Grim (40.7°S, 144.7°E) are shown in Figure 2. Regional background concentrations of CH₃Br
120 were determined by removing pollution events after applying a polynomial fit to the lower 99.7% (within 3σ) of the Gaussian distribution derived from the 121-day observations for 60 days before and after each observed data point (O’Doherty et al., 2001). The baseline concentrations at Gosan and Mace Head (northern hemisphere) are higher than those of Cape Grim (southern hemisphere), and while the annual cycles at Gosan and Mace Head are similar.

The annual average CH₃Br baseline concentrations decreased steadily from 8.5 ± 0.8 ppt in 2008 to 7.4 ± 0.6 ppt in 2019
125 (Table 1), declining at a rate of -0.13 ± 0.02 ppt yr⁻¹ (-1.5% yr⁻¹). This rate of decline for CH₃Br is consistent with the global trend of atmospheric CH₃Br determined from AGAGE *in situ* and NOAA (National Oceanic and Atmospheric Administration) flask data in 2011–2012 (Carpenter and Reimann et al., 2014), which has been attributed to the influence of the CH₃Br restrictions on non-QPS use imposed by the Montreal Protocol.



130 The monthly mean CH₃Br baseline concentrations for 2008–2019 are shown in Figure 3. The seasonal variations show a steady increase in spring, reaching a maximum in May, then dropping in June–July, followed by a constant level for the last 5 months of the year. The various sources and sinks of CH₃Br likely show seasonal variability, and the summertime minima in CH₃Br can be largely explained by the atmospheric concentrations of OH reaching a maximum during the boreal summer (Cox, 2002; Simmonds et al., 2004) and long-range transport of southern hemispheric air parcel that over-cross the tropical regions (Li et al., 2018).

135 Despite the continuous decrease in background concentrations, we observed clear pollution signals (shown in red in Figure 2) through the entire study period, representing persistent inflow to Gosan of air masses influenced by regional CH₃Br emission sources and thus containing elevated concentrations of CH₃Br. The annual means of the enhancement concentrations (pollution – baseline) are consistently in a range of 3.5 to 5.0 ppt as given in Figure 4. Note that there are data missing for several months in 2016, 2017, and 2018, mainly because of typhoon damage to the Gosan station in early summer/fall.

140 **4 Potential CH₃Br source regions**

The regional distribution of potential CH₃Br sources in East Asia was derived by applying a statistical analysis of back trajectories corresponding to the observed CH₃Br enhancements at Gosan from 2008 to 2019. Air mass back trajectories were generated using the Hybrid Single-Particle Lagrangian Integrated Trajectory (HYSPPLIT; Draxler et al., 1998) model from the NOAA Air Resources Laboratory with meteorological data output from the Global Data Assimilation System (1°×1° horizontal resolution, 23 vertical layers, <ftp://arlftp.arlhq.noaa.gov/pub/archives/gdas1>). The HYSPLIT 6-day air mass backward trajectories were initialized 500 m above the Gosan observation station, at a height where topographical influences can be minimized (Li et al., 2014). To minimize the error that arises from a small number of outlier trajectories, only grids with more than 12 over-passing trajectories were used to define a potential source region (Reimann et al., 2004; method described in SI). Figure 5 shows the distribution of potential CH₃Br source regions in East Asia for 2008–2019, widely distributed over eastern China and southern Korea. In particular, high potential source regions for CH₃Br emissions are seen along the Yangtze River that connects Shanghai, Nanjing, Hefei and Wuhan. The port of Shanghai is one of the busiest container ports in the world since 2010, with high volumes of port traffic and a large population (Robert et al., 2020). For example, Shanghai handled 43.3 million twenty-foot equivalent units in 2019 (<https://safety4sea.com/port-of-shanghai-worlds-busiest-container-port-for-2019/>, last access: 11 March, 2021). In several cases, high CH₃Br concentrations were observed in narrow-width air mass back trajectories that showed long residence times over the port of Shanghai (see Figure S1), which would be consistent with Shanghai being a likely major port for QPS usage of CH₃Br.

155 The high potential source regions include not only modern industrial urban areas but also the vast alluvial plains along the Yangtze River and its main tributaries. Note that this statistical analysis has little sensitivity to emissions from southwestern China and tends to over-estimate source strengths near the boundary due to the limits of the 5–6 day backward trajectory domain of the HYSPLIT model. Therefore, those parts of China have been excluded from further discussion (Park

160



et al., 2018). Also note that this statistical trajectory analysis tends to underestimate emissions at sub-grid scale hotspots because the measured concentration gets distributed evenly over the grid cell (Stohl, 1996). Also, the dilution effects on distant source emissions are not considered in this statistical approach (Vollmer et al., 2006). Thereby, the emissions from nearby sources might be overestimated due to the higher CH₃Br concentration. For this reason, the emission potential for South Korea, shown in Figure 5, may be lower. We do not attempt to identify more exact locations of CH₃Br emission sources based on this approach because of its potential uncertainties, nevertheless it is clear that significant emissions of CH₃Br originate predominantly from eastern-central China.

5 Estimation of CH₃Br Emissions from eastern China using an inter-species correlation method

In the previous section, it was noted that most of the air masses exhibiting enhanced CH₃Br concentrations flow into Gosan from eastern China. We classify the air mass origins into 17 regions (see Figure S2a for the regional domains) based on the 6-day kinematic back trajectories of the HYSPLIT model. If a trajectory arriving at Gosan had entered the boundary layer (as defined by HYSPLIT) only within the regional domains for eastern China-1 (region 16), eastern China-2 (region 5), and Shandong provinces (region 9), it was defined as an air mass originating from eastern China. The air mass classification applied to the CH₃Br time series is illustrated in Figure S2b. The proportions of CH₃Br pollution events from 2008 to 2019 classified into China, South Korea, and other regions were 37, 44, and 19%, respectively. Among them, 98% of air masses classified as China correspond to eastern China (~35% of the total).

5.1 Interspecies correlation method

To estimate emission of CH₃Br from eastern China, we applied an interspecies correlation (ISC) method (Palmer et al., 2003; Dunse et al., 2005; Yokouchi et al., 2006; Millet et al., 2009; Li et al., 2011; Wang et al., 2014; Park et al., 2018). Described as a “ratio-method”, this approach can derive the emission of a trace gas of interest from the correlation of its enhancement above baseline with that of a reference compound. This empirical ratio approach can estimate regional emissions of various substances in a simple and robust manner, compared to inverse methods that require complex computational processes in combination with chemical transport models. For a reference tracer in ISC method, the following conditions are required: i) long lifetime, thus low chemical reactivity during transport from source to observation site, ii) well-quantified emission sources, iii) approximate co-location of the source regions for the reference and target species resulting in significant correlations with the target species. Several previous studies have used carbon monoxide (CO) as a reference species for ISC (Palmer et al., 2003; Dunse et al., 2005; Guo et al., 2009; Wang et al., 2014). CO can be observed readily at the target species observation sites and often has documented emissions from anthropogenic sources, usually as a component of regional air quality emissions inventories. One of the issues of using CO as a reference species in ISC is that the emission inventories usually document anthropogenic CO sources only, whereas the observations see CO emissions from anthropogenic and natural sources, biomass



burning for example. Therefore, in the CO observational data record, CO pollution episodes have to be identified as predominantly anthropogenic before inclusion in the ISC emissions calculations, which complicates matters.

Instead, we selected CFC-11 as the reference compound, because CFC-11 has a long lifetime (50–60 years) with low chemical reactivity, has been measured simultaneously with CH₃Br at Gosan showing strong correlations (Li et al., 2011), and the CFC-11 emissions from eastern China for 2008–2019 have been very well-quantified by four different inverse models (Rigby et al., 2019; Park et al. 2021).

Atmospheric observations of CH₃Br, CFC-11, benzene, toluene and ethane (Figure 6), show significant correlations between CH₃Br and CFC-11, for example on 19 and 21 May. The volatile organic compounds (VOCs), like benzene, toluene and ethane, are emitted from biomass burning, show a noteworthy simultaneous increment, suggesting that biomass burning in eastern China could be a potential CH₃Br source. This point is discussed in detail in the next session.

The emissions of CFC-11 are from anthropogenic sources only – there are no natural sources of CFC-11. Although the emission sources of CFC-11 and CH₃Br are not necessarily co-located on an emission activity basis, we can still apply ISC method to estimate the magnitude of country/regional scale emissions of CH₃Br, when they occur within a same country/region where CFC-11 is emitted. When the likely CFC-11 and CH₃Br sources are not co-located on a fine scale but are co-located on a regional scale, then it is important to make the CFC-11 and CH₃Br observations sufficiently distant (hundreds of km) from the source region so that the initial individual plumes of CFC-11 and CH₃Br emissions from separate sources become well mixed. In this study, the emissions of CH₃Br in eastern China are derived using the following equation:

$$E_{MB} = E_{CFC-11} \times \alpha \times \frac{M_{MB}}{M_{CFC-11}}, \quad (1)$$

210

where, E_{MB} and E_{CFC-11} are the emissions of CH₃Br and CFC-11, respectively, α is a slope of linear regression between enhancements of CH₃Br and CFC-11 (Δ CH₃Br and Δ CFC-11), M_{MB} and M_{CFC-11} are the molecular weights of CH₃Br and CFC-11, respectively. The intercept term of the linear regression can be ignored because it is generally not significantly different than zero, confirmed by the similar slope terms from linear and linear-through-the-origin regressions (Dunse et al., 2005).

215

The uncertainty of CH₃Br emissions is associated with uncertainties of α and E_{CFC-11} and determined by an error propagation method as follows:

$$\sigma E_{MB} = \sigma E_{CFC-11} + \sigma \alpha \quad (2)$$

220

where, σE_{MB} is the uncertainty of estimated CH₃Br emissions, σE_{CFC-11} and $\sigma \alpha$ are the uncertainties of E_{CFC-11} and α , respectively.



5.2 CFC-11 emissions from inverse model frameworks

We use known emission estimates of CFC-11 from eastern China, which were derived by inverse modelling of Gosan CFC-11 observation data (Rigby et al., 2019; Park et al., 2021). Atmospheric concentrations for CFC-11 observed over the same period with CH₃Br are shown in Figure S3. CFC-11 emissions were estimated from four different Bayesian inverse methods based on two different Lagrangian atmospheric chemical transport models: the UK Met Office Numerical Atmospheric-dispersion Modelling Environment (NAME; Jones et al., 2007) and the FLEXible PARTicle dispersion model (FLEXPART; Stohl et al., 2005; Pisso et al., 2019). The details for the modelling frameworks are described in Rigby et al. (2019) and Park et al. (2021). For E_{CFC-11} and σ_{CFC-11} in Eq. 1 and 2, the emissions of CFC-11 and their uncertainties are derived from the four inversion models used (Park et al., 2021). The average value of estimated emissions of CFC-11 for eastern China ranged from 5.7 to 20.4 Gg yr⁻¹ over the period 2008–2019 (Park et al., 2021).

5.3 Linear regression

Several studies have used ordinary least squares (OLS) as a linear regression method due to its simplicity. With OLS, the errors of both independent variables are not considered. However, if both variables have uncertainties like the observation data used in this study, both errors must be considered when performing a linear regression between the two variables. Some other linear regression methods considering the XY errors have been suggested to overcome the limitation of OLS. Dunse et al. (2005) used the Fitexy method (Press et al., 2007), Wang et al. (2014) used the Orthogonal Distance regression (ODR; Wallace et al., 2012), and Park et al. (2018) used the Williamson-York regression (WYR; Cantrell, 2008) to estimate the emissions of the trace gases by ISC method. A recent study (Wu and Yu, 2018) suggested that Weighted Deming Regression (WDR; hereafter, DR) method estimates a relatively more accurate slope and intercept by minimizing the residual errors both X and Y among the various linear regression methods, particularly for atmospheric data with measurement error. As mentioned earlier, the calculated slopes can be different depending on which linear regression fit is used. Therefore, we applied not only the DR approach but also the Fitexy and WYR methods to determine annual slopes between the observed enhancements of CH₃Br and CFC-11 during 2008 to 2019. The results for the Fitexy and WYR methods are similar. Even though the co-matched observation points were slightly scattered in the range of large enhancements, the DR generated best fits representing the overall correlations trends. Millet et al. (2009) required a Pearson correlation coefficient (R) over 0.3. Figure S4 shows the resulting annual slopes. For most of entire observation period, CH₃Br enhancements show a significant correlation with those for CFC-11 with R larger than 0.4 (e.g., R = 0.7 in 2009). They do not maintain a high correlation (R < 0.4) for every single year since most of the enhancements of CH₃Br and CFC-11 were less than 5 ppt and high pollution events occurred only occasionally within a year. Nevertheless, CFC-11 seems suitable as a reference compound to trace anthropogenic emissions from eastern China.



5.4 Estimation of CH₃Br emissions from eastern China

Figure 7 shows the annual CH₃Br emissions estimates derived for eastern China by ISC method from atmospheric
255 measurements at Gosan from 2008 to 2019. The bar plots represent annual CH₃Br emissions with 1- σ uncertainties, which
were determined based on CFC-11 emissions derived from four different inversion frameworks. The results derived from
different inversion methods agree within the stated uncertainties for most years. Note that the emissions estimate in 2013
calculated from the NAME-HB CFC-11 inversion was 2.6 Gg yr⁻¹, while those from other inversions were larger than 5 Gg
yr⁻¹. Despite the uncertainty ranges for the CFC-11 inversion results and for the least-squares fits in the ISC method, the
260 resulting CH₃Br emissions from eastern China have remained relatively constant at 4.1 ± 1.3 Gg yr⁻¹ for the period 2008–2019,
with small fluctuations from year to year. This represents 40–50% of the summed global emissions of CH₃Br for QPS (on
average of 8.0 Gg yr⁻¹) and non-QPS (on average of 2.2 Gg yr⁻¹) fumigation usage in 2008–2019 (see Table S2; Carpenter and
Reimann et al., 2014; TEAP, 2020).

The emissions of CH₃Br peaked in 2010 at 7.1 ± 1.3 Gg yr⁻¹ and then decreased to 2.4 ± 1.3 ppt in 2012, followed by a slight
265 increasing trend in later years. The abrupt increase of CH₃Br emissions in 2010 is difficult to explain in terms of the
consumption and production data reported to the Ozone Secretariat for both controlled uses and QPS uses of CH₃Br. The
consumption in 2010 and 2012 was less than 1.5 Gg yr⁻¹ and possible emissions between 1.0 – 1.4 Gg yr⁻¹. The cause(s) of the
relatively large emissions in 2010 and 2013 are unknown. One possibility is wildfire CH₃Br emissions from China modulated
by the El Niño-Southern Oscillation (ENSO). South-western China showed an ENSO-related maximum in fire occurrences in
270 2010 and south-eastern China in 2013 (Fang et al., 2021). The increase in CH₃Br emissions for 2014–2018 possibly reflects
the impact of increased QPS CH₃Br use in traded commodities as reported to UNEP (MBTOC, 2018).

Figure 8 shows the comparison between bottom-up emissions of CH₃Br for China reported to UNEP and top-down emissions
of CH₃Br derived by ISC for eastern China using CFC-11 as the reference emissions. The detailed values of each category
are described in Table 2. The bottom-up emissions of CH₃Br used in fumigation are determined by applying an emission factor
275 of 65% to the reported non-QPS consumption and 84% to the reported QPS consumption (MBTOC, 2006).

As mentioned earlier, the increase in bottom-up emissions of CH₃Br over the period 2014–2018 is consistent with an increase
in consumption for QPS fumigation. However, in 2019, the reported non-QPS and QPS consumptions were reduced to zero
and 0.87 Gg yr⁻¹, respectively. The total calculated emissions of CH₃Br in 2019 (0.73 Gg yr⁻¹) are lower than in 2008 (1.44 Gg
yr⁻¹). The average of the bottom-up emissions of CH₃Br from China is 1.1 ± 0.2 Gg yr⁻¹ in the period of 2008–2019.

280 5.5 Potential of anthropogenic sources that contribute to CH₃Br emissions

Overall, the variations of both bottom-up and top-down emissions exhibit qualitative agreement, with peak emissions in 2010,
a decrease in 2011 and 2012 and a slight increase until 2017 and 2018 (except for the large top-down emissions in 2010 and
2013 discussed above), and then decreasing again in 2019. However, there is an obvious, significant discrepancy between the
absolute values of both data sets. Considering the bottom-up emissions were based on reported data for all of China and the



285 top-down emissions were derived for eastern China, actual difference in derived emissions of CH_3Br is likely to be larger. Assuming that the emissions from eastern China represent the entire Chinese emissions, the mean difference between the bottom-up and top-down estimates over the entire period 2008–2019 is $2.9 \pm 1.3 \text{ Gg yr}^{-1}$. The largest difference was in 2010 (5.8 Gg yr^{-1}), with top-down emissions (7.1 Gg) nearly a factor of 6 times greater than the bottom-up emissions (1.2 Gg). The causes of these large discrepancies in estimated emissions of CH_3Br are not obvious.

290 We have examined some possibilities –

(i) Rapeseed industry

In the life cycle of rapeseed, CH_3Br is largely emitted during the flowering period in the 2 months after sowing (Jiao et al., 2020). Rapeseed in the northern hemisphere generally blooms in the warm weather from March to May. So seasonal emissions from the arable land of rapeseed may be related to the observed springtime increase in CH_3Br polluted concentrations at Gosan
295 (See Figure S5).

China is the third-largest producer of rapeseed in the world after the European Union and Canada, accounting for 12% of the total rapeseed production in 2015–2016, and the arable land lies mainly along the Yangtze River, which is suitable for growing rapeseed (Khir et al., 2017). Previous studies have reported that the global emissions of CH_3Br by the rapeseed industry range from $2.8 \pm 0.7 \text{ Gg yr}^{-1}$ (Jiao et al., 2020) to 5 Gg yr^{-1} (Gan et al., 1998; Mead et al., 2008). Considering the proportion of eastern
300 China in global rapeseed industry, the emissions of CH_3Br by rapeseed in eastern China could be about $0.3\text{--}0.6 \text{ Gg yr}^{-1}$.

(ii) Biomass burning

Owing to the almost total phase out of CH_3Br for non-QPS uses to date, the largest contributor to global anthropogenic emissions of CH_3Br is biomass burning, such as agricultural open-field burning and use of biofuels (about 23 Gg yr^{-1} ; Carpenter and Reimann et al., 2014). As shown in Figure 6, the elevated concentrations of VOCs (toluene, benzene, ethane), which are
305 associated with biomass burning, are correlated with elevated concentrations of CH_3Br , suggesting that there may be some contribution of biomass burning to the observed CH_3Br enhancements. Note, the sources of VOCs pollution are generally not entirely due to biomass burning, as VOCs are emitted by combustion processes in general (e.g., fossil fuel use and combustion). Approximately 140 Tg of agricultural residues are burned in fields across all of China every year (Zhao et al., 2017). Biomass burning in eastern China is predominantly due to the burning of agricultural crop residues ($\sim 60 \text{ Tg yr}^{-1}$), mainly wheat residues
310 (in May–June), rice and corn residues (in September–October) (Zhang et al., 2020). This eastern China biomass burning seasonality may contribute partly to the seasonality in elevated levels of CH_3Br seen at Gosan (May–June and September–October, see Figure S5).

The global annual emissions of CH_3Br from the burning of agricultural waste are uncertain. Recently, Andreae (2019) has revised the emission factor (EF) of CH_3Br by agricultural residues from the field experiment to $1.1 \text{ g tonnes}^{-1}$, and based on
315 this, the global biomass burning emission of CH_3Br by agricultural residues estimates was 0.3 Gg yr^{-1} . Using this EF, the emissions of CH_3Br from biomass burning of agricultural residues in eastern China would be approximately 0.07 Gg yr^{-1} .

(iii) Post-harvest treatment



Historically, CH₃Br consumption results from soil fumigation (non-QPS), structural fumigation (non-QPS) and post-harvest fumigation (mainly QPS). Currently, the phase-out of CH₃Br has been successfully implemented under the Montreal Protocol for non-QPS applications, in particular the decrease in consumption of CH₃Br for soil fumigation. Chemicals (e.g., chloropicrin, metam sodium, dazomet, etc.) and non-chemical methods (steam, soilless culture, resistant varieties) have been successfully introduced as alternatives to CH₃Br use as soil fumigants (Mao et al., 2016; MBTOC, 2018). For QPS applications, phosphine has been widely used as a substitute for CH₃Br in post-treatment of commodities, but it is known that some pests have developed resistance to phosphine (Jagadeesan and Nayak, 2017; Xinyi et al., 2017). SO₂F₂ is used in China as an alternative to non-QPS use of CH₃Br for the pre-plant soil fumigation as well as the QPS disinfestation of some durable products and post-harvest commodities (Cao et al., 2014; Gressent et al., 2021). Interestingly, the spatial distribution of the potential emission source regions estimated from the SO₂F₂ pollution observed at Gosan is very similar to that for CH₃Br (Figure S6). In addition, the concentrations of SO₂F₂ and CH₃Br increase contemporaneously, and the correlations between the enhancements of both substances and CFC-11 are significant (Figure S7 and S8). This implies temporal and spatial co-emissions of SO₂F₂ with anthropogenic CH₃Br into the atmosphere. Gressent et al. (2021) showed that SO₂F₂ emissions in China were predominantly generated by post-harvest treatment rather than structural fumigation and were distributed within a large portion in East China. Using these Gressent et al. SO₂F₂ emissions, the CH₃Br emissions from eastern China for post-harvest treatment derived by the ISC method from the observations of SO₂F₂ and CH₃Br at Gosan were 0.9 ± 0.2 Gg yr⁻¹ for the period 2014–2019. Thus, the post-harvest use of CH₃Br in eastern China results in approximately 1 Gg yr⁻¹ of anthropogenic CH₃Br emissions.

(iv) Unreported or inaccurately reported emissions from fumigation usage

The CH₃Br emissions proposed above in (i)–(iii) can account for about half of the discrepancy (2.9 Gg yr⁻¹) between ‘top down’ and ‘bottom up’ estimates for east China. The sources of the remaining discrepancies (~1.4 Gg yr⁻¹) in CH₃Br emissions remain unknown.

Errors in the reported inventory for regulated uses cannot be ruled out because it is unsure whether the limits on new QPS use have been adhered to (MBTOC, 2018). Besides, despite the successful reduction of anthropogenic CH₃Br emissions globally, the possibility of unidentified sources of emissions has been raised in multi-year MBTOC assessment reports (Porter and Fraser, 2020). As a similar example, we note that, although CFC-11 was a very important target chemical for phase-out under the Montreal Protocol, unexpected CFC-11 emission increases were found due to unreported production and use in eastern China during 2013–2018 (Rigby et al., 2019; Park et al., 2021). In addition, it may be premature to conclude that CH₃Br non-QPS use in China has been completely replaced by the alternatives discussed above. Since CH₃Br represents the most effective and the cheapest fumigation method, the transition to the use of alternatives may be delayed without strong regulations and/or financial incentives and/or social awareness. The fact that CH₃Br emissions derived from atmospheric observations in this study are significantly larger than reported emissions suggests that unreported fumigation use of CH₃Br may have occurred during the transition to alternative fumigation methods or that other sources, such as emissions from industrial wastes, have been overlooked.



6 Summary and conclusion

Atmospheric CH₃Br has both natural and anthropogenic sources and plays a significant role in stratospheric ozone destruction. For this reason, CH₃Br non-QPS uses as a soil, commodity treatment and structural fumigant are being phased-out globally under the Montreal Protocol on Substances that Deplete the Ozone Layer, and its QPS use as a commodity fumigant is regulated. To understand the temporal trend in atmospheric CH₃Br abundances and its emission sources in East Asia, we analyzed the concentrations of CH₃Br observed at Gosan (Jeju Island, South Korea) for 12 years from 2008 to 2019. The baseline concentrations indicating the regional state of the background atmosphere have decreased by -0.13 ± 0.02 ppt yr⁻¹ (-1.5 % yr⁻¹) during the period, with seasonal variations increasing in spring and decreasing in summer. Despite the decreasing trend of the CH₃Br baseline, relatively constant-strength pollution events occurred in every year.

A statistical backward trajectory analysis showed that emissions of CH₃Br in the region were highest from eastern China compared to other surrounding countries. Top-down emissions estimates of CH₃Br from eastern China were determined by using an ISC method with CFC-11 as the reference tracer defining anthropogenic CH₃Br emissions. The ISC-based CH₃Br emission rates were 4.1 ± 1.3 Gg yr⁻¹ on average during 2008–2019 and, despite the CH₃Br phase-out for non-QPS applications in Article 5 countries, which includes China, in 2015, significant CH₃Br emissions have continued. These CH₃Br emissions determined from atmospheric observations are significantly different from the bottom-up emission estimates predicted from consumption data reported to UNEP (1.1 ± 0.2 Gg yr⁻¹). The possible contributions of rapeseed production and biomass burning to this discrepancy were assessed at approximately 0.6 ± 0.2 Gg yr⁻¹, insufficient to explain the approximate 3 Gg yr⁻¹ difference between top-down (4.1 Gg yr⁻¹) and bottom-up (1.1 Gg yr⁻¹) estimates.

The remaining discrepancy (3.5 Gg yr⁻¹) is most likely due to fumigation use that was not reported and/or inaccurately reported or emissions from unknown sources, such as industrial waste or other sources. Correlations between CH₃Br and SO₂F₂ pollution levels at Gosan suggest that the post-harvest use of CH₃Br in eastern China contributes 0.9 ± 0.2 Gg yr⁻¹ to this 3.5 Gg yr⁻¹ discrepancy. These data may suggest that the transition from CH₃Br to SO₂F₂ or other alternatives for post-harvest fumigation in eastern China is only partially complete. Unreported use for fumigation may be related to the delay in introducing alternative technologies to CH₃Br fumigation in east China and/or the lack of social awareness of the regulation, during the transitional period to alternative technologies.

Most of our estimated emissions of CH₃Br are from eastern China and these CH₃Br emissions, likely from unreported or inaccurately reported fumigation usage, are significant enough to account for 30–40% of global emissions for fumigation usage. Further analysis of CH₃Br emissions from all of China would enhance understanding of these potentially unreported/underestimated emissions. Our method has limitations in considering all sources of CH₃Br and thus inherent uncertainties. Nevertheless, it is important to investigate the accuracy of bottom-up emission inventories for anthropogenic sources of CH₃Br using comparisons with observation-derived top-down emissions estimates as presented here.



The total tropospheric bromine (in units of ppt) from long-lived brominated substances (CH₃Br and halons) controlled by the
385 MP has been decreasing since reaching a peak in 1998, mainly due to the decline of CH₃Br. However, the contributions of
halons to declining tropospheric bromine have become predominant since 2012 (Carpenter and Reimann et al., 2014). In recent
years, CH₃Br accounts for a significant proportion of the total amount of bromine in the troposphere from long-lived
compounds. Consequently, if any unreported non-QPS and QPS emissions from fumigation usage could be reduced and
eventually stopped in developing countries, a further reduction of atmospheric CH₃Br concentrations would occur very quickly,
390 due to the short half-life of CH₃Br. For this reason, continued monitoring of atmospheric CH₃Br concentrations in East Asia
and improvements in inverse modelling approaches are presently seen as a key priority in order to locate and identify specific
emission sources.

Data availability

Data used in this study are available from the AGAGE (Advanced Global Atmospheric Gases Experiment) database
395 (http://agage.eas.gatech.edu/data_archive/agage/gc-ms-medusa/, last access: August 2021)

Author contributions

HC, SP, and PJF designed the study; HC, SP, PJF, IP, JM, and JK interpreted the analyzed results and wrote the manuscript;
HC, SP, MP, HP, and SG carried out the measurement of CH₃Br and CFC-11 at Gosan; JM, PKS, CMH and RFW supported
the calibration and long-term precision for the observations at Gosan; SOD and DY provided the *in situ* measurement data
400 from Mace Head; PJF, BLD, and PBK provided the *in situ* measurement data from Cape Grim.

Competing interests

The authors declare that they have no conflict of interest.

Acknowledgements

This research was supported by the National Research Foundation of Korea (NRF) grant funded by the Korean government
405 (MSIT) (no. 2020R1A2C3003774). Support for contributions by J. Kim, J. Mühle, C. M. Harth, P. K. Salameh, and R. F.
Weiss came from National Aeronautics and Space Administration (grant nos. NNX16AC96G and NNX16AC97G). Support
for contributions by P. J. Fraser, B. L. Dunse, and P. B. Krummel came from National Aeronautics and Space Administration
(grant no. NNX16AC98G), the Australian Bureau of Meteorology, CSIRO, the Australian Department of Agriculture, Water
and the Environment (DAWE). Support for contributions by I. Porter funded by La Trobe University.



410 References

- Andreae, M. O. and Merlet, P.: Emission of trace gases and aerosols from biomass burning, *Global Biogeochem. Cycles*, doi:10.1029/2000GB001382, 2001.
- Andreae, M. O.: Emission of trace gases and aerosols from biomass burning - An updated assessment, *Atmos. Chem. Phys.*, doi:10.5194/acp-19-8523-2019, 2019.
- 415 Blake, N. J., Blake, D. R., Simpson, I. J., Meinardi, S., Swanson, A. L., Lopez, J. P., Katzenstein, A. S., Barletta, B., Shirai, T., Atlas, E., Sachse, G., Avery, M., Vay, S., Fuelberg, H. E., Kiley, C. M., Kita, K. and Rowland, F. S.: NMHCs and halocarbons in Asian continental outflow during the Transport and Chemical Evolution over the Pacific (TRACE-P) field campaign: Comparison with PEM-West B, *J. Geophys. Res. Atmos.*, doi:10.1029/2002jd003367, 2003.
- Cantrell, C. A.: Technical Note: Review of methods for linear least-squares fitting of data and application to atmospheric chemistry problems, *Atmos. Chem. Phys.*, doi:10.5194/acp-8-5477-2008, 2008.
- 420 Cao, A., Guo, M., Yan, D., Mao, L., Wang, Q., Li, Y., Duan, X. and Wang, P.: Evaluation of sulfuryl fluoride as a soil fumigant in China, *Pest Manag. Sci.*, doi:10.1002/ps.3535, 2014.
- Carpenter, L. J., Reimann, S., Burkholder, J. B., Clerbaux, C., Hall, B. D., Hossaini, R., Laube, J. C., Yvon-Lewis, S. A., Blake, D. R., Dorf, M., Dutton, G. S., Fraser, P. J., Froidevaux, L., Hendrick, F., Hu, J., Jones, A., Krummel, P. B., Kuijpers, L. J.
- 425 M., Kurylo, M. J., Liang, Q., Mahieu, E., Mühle, J., O'Doherty, S., Ohnishi, K., Orkin, V. L., Pfeilsticker, K., Rigby, M., Simpson, I. J., Yokouchi, Y., Engel, A., and Montzka, S. A.: Update on Ozone-Depleting Substances (ODS) and Other Gases of Interest to the Montreal Protocol (Chapter 1), in: *Scientific Assessment of Ozone Depletion: 2014*, Global Ozone Research and Monitoring Project-Report No. 55, World Meteorological Organization, Geneva, Switzerland, 2014.
- Cox, M.L., 2002. A regional study of the natural and anthropogenic sources and sinks of the major halomethanes. Ph.D. Thesis, Monash University, School of Mathematical Sciences, Clayton, Victoria, Australia.
- 430 Cunnold, D. M., Fraser, P. J., Weiss, R. F., Prinn, R. G., Simmonds, P. G., Miller, B. R., Alyea, F. N. and Crawford, A. J.: Global trends and annual releases of CCl₃F and CCl₂F₂ estimated from ALE/GAGE and other measurements from July 1978 to June 1991, *J. Geophys. Res.*, doi:10.1029/93jd02715, 1994.
- Draxler, R. R. and Hess, G. D.: An overview of the HYSPLIT_4 modelling system for trajectories, dispersion and deposition, 435 *Aust. Meteorol. Mag.*, 1998.
- Dunse, B. L., Steele, L. P., Wilson, S. R., Fraser, P. J. and Krummel, P. B.: Trace gas emissions from Melbourne, Australia, based on AGAGE observations at Cape Grim, Tasmania, 1995-2000, *Atmos. Environ.*, doi:10.1016/j.atmosenv.2005.07.014, 2005.
- Engel, A. and Rigby, M., Burkholder, J. B., Fernandez, R. P., Froidevaux, L., Hall, B. D., Hossaini, R., Saito, T., Vollmer, M.
- 440 K., and Yao, B.: Update on Ozone-Depleting Substances (ODS) and Other Gases of Interest to the Montreal Protocol, Chap. 1, in: *Scientific Assessment of Ozone Depletion: 2018*, Global Ozone Research and Monitoring Project-Report No. 58, World Meteorological Organization, Geneva, Switzerland, 2019.



- Fang, K., Yao, Q., Guo, Z., Zheng, B., Du, J., Qi, F., Yan, P., Li, J., Ou, T., Liu, J., He, M. and Trouet, V.: ENSO modulates wildfire activity in China, *Nat. Commun.*, doi:10.1038/s41467-021-21988-6, 2021.
- 445 Gan, J., Yates, S. R., Ohr, H. D. and Sims, J. J.: Production of methyl bromide by terrestrial higher plants, *Geophys. Res. Lett.*, doi:10.1029/98gl52697, 1998.
- Gressent, A., Rigby, M., Ganesan, A. L., Prinn, R. G., Manning, A. J., Mühle, J., Salameh, P. K., Krummel, P. B., Fraser, P. J., Steele, L. P., Mitrevski, B., Weiss, R. F., Harth, C. M., Wang, R. H., O'Doherty, S., Young, D., Park, S., Li, S., Yao, B., Reimann, S., Vollmer, M. K., Maione, M., Arduini, J. and Lunder, C. R.: Growing Atmospheric Emissions of Sulfuryl Fluoride, 450 *J. Geophys. Res. Atmos.*, doi:10.1029/2020JD034327, 2021.
- Guo, H., Ding, A. J., Wang, T., Simpson, I. J., Blake, D. R., Barletta, B., Meinardi, S., Rowland, F. S., Saunders, S. M., Fu, T. M., Hung, W. T. and Li, Y. S.: Source origins, modeled profiles, and apportionments of halogenated hydrocarbons in the greater Pearl River Delta region, southern China, *J. Geophys. Res. Atmos.*, doi:10.1029/2008JD011448, 2009.
- Hu, L., Yvon-Lewis, S., Liu, Y. and Bianchi, T. S.: The ocean in near equilibrium with atmospheric methyl bromide, *Global* 455 *Biogeochem. Cycles*, doi:10.1029/2011GB004272, 2012.
- Jagadeesan, R. and Nayak, M. K.: Phosphine resistance does not confer cross-resistance to sulfuryl fluoride in four major stored grain insect pests, *Pest Manag. Sci.*, doi:10.1002/ps.4468, 2017.
- Jiao, Y., Acdan, J., Xu, R., Deventer, M. J., Zhang, W. and Rhew, R. C.: Global Methyl Halide Emissions From Rapeseed (*Brassica napus*) Using Life Cycle Measurements, *Geophys. Res. Lett.*, doi:10.1029/2020GL089373, 2020.
- 460 Jones, A. R., Thomson, D. J., Hort, M. C. and Devenish, B.: The U.K. Met Office's Next-Generation Atmospheric Dispersion Model, NAME III BT - Air Pollution Modeling and Its Application XVII, in *Air Pollution Modeling and Its Application XVII*, 2007.
- Khair, K.A., Ismail, N., Balu, N.: Competitiveness of the rapeseed industry in China, *Oil Palm Industry Econ. J.*, 2017.
- Kim, J., Li, S., Mühle, J., Stohl, A., Kim, S. K., Park, S., Park, M. K., Weiss, R. F. and Kim, K. R.: Overview of the findings 465 from measurements of halogenated compounds at Gosan (Jeju Island, Korea) quantifying emissions in East Asia, *J. Integr. Environ. Sci.*, doi:10.1080/1943815X.2012.696548, 2012.
- Lee-Taylor, J. M. and Holland, E. A.: Litter decomposition as a potential natural source of methyl bromide, *J. Geophys. Res. Atmos.*, doi:10.1029/1999JD901112, 2000.
- Lee-Taylor, J. M., Brasseur, G. P. and Yokouchi, Y.: A preliminary three-dimensional global model study of atmospheric 470 methyl chloride distributions, *J. Geophys. Res. Atmos.*, doi:10.1029/2001JD900209, 2001.
- Li, S., Kim, J., Kim, K. R., Mühle, J., Kim, S. K., Park, M. K., Stohl, A., Kang, D. J., Arnold, T., Harth, C. M., Salameh, P. K. and Weiss, R. F.: Emissions of halogenated compounds in east asia determined from measurements at Jeju Island, Korea, *Environ. Sci. Technol.*, doi:10.1021/es104124k, 2011.
- Li, S., Kim, J., Park, S., Kim, S. K., Park, M. K., Mühle, J., Lee, G., Lee, M., Jo, C. O. and Kim, K. R.: Source identification 475 and apportionment of halogenated compounds observed at a remote site in East Asia, *Environ. Sci. Technol.*, doi:10.1021/es402776w, 2014.



- Li, S., Park, S., Lee, J. Y., Ha, K. J., Park, M. K., Jo, C. O., Oh, H., Mühle, J., Kim, K. R., Montzka, S. A., O'Doherty, S., Krummel, P. B., Atlas, E., Miller, B. R., Moore, F., Weiss, R. F. and Wofsy, S. C.: Chemical evidence of inter-hemispheric air mass intrusion into the Northern Hemisphere mid-latitudes, *Sci. Rep.*, doi:10.1038/s41598-018-22266-0, 2018.
- 480 Manley, S. L., Wang, N. Y., Walser, M. L. and Cicerone, R. J.: Methyl halide emissions from greenhouse-grown mangroves, *Geophys. Res. Lett.*, doi:10.1029/2006GL027777, 2007.
- Mao, L., Wang, Q., Yan, D., Li, Y., Ouyang, C., Guo, M. and Cao, A.: Flame soil disinfection: A novel, promising, non-chemical method to control soilborne nematodes, fungal and bacterial pathogens in China, *Crop Prot.*, doi:10.1016/j.cropro.2016.02.002, 2016.
- 485 Mead, M. I., White, I. R., Nickless, G., Wang, K. Y. and Shallcross, D. E.: An estimation of the global emission of methyl bromide from rapeseed (*Brassica napus*) from 1961 to 2003, *Atmos. Environ.*, doi:10.1016/j.atmosenv.2007.09.020, 2008.
- Methyl Bromide Technical Options Committee (MBTOC): Report of the Methyl Bromide Technical Options Committee: 2006 assessment. United Nations Environment Program, Nairobi, Kenya, 2006.
- MBTOC (Methyl Bromide Technical Options Committee): Report of the Methyl Bromide Technical Options Committee: 490 2018 Assessment, United Nations Environment Program, Nairobi, Kenya, 2018.
- Miller, B. R., Weiss, R. F., Salameh, P. K., Tanhua, T., Grealley, B. R., Mühle, J. and Simmonds, P. G.: Medusa: A sample preconcentration and GC/MS detector system for in situ measurements of atmospheric trace halocarbons, hydrocarbons, and sulfur compounds, *Anal. Chem.*, doi:10.1021/ac702084k, 2008.
- Millet, D. B., Atlas, E. L., Blake, D. R., Blake, N. J., Diskin, G. S., Holloway, J. S., Hudman, R. C., Meinardi, S., Ryerson, T. 495 B. and Sachse, G. W.: Halocarbon emissions from the United States and Mexico and their global warming potential, *Environ. Sci. Technol.*, doi:10.1021/es802146j, 2009.
- Montzka, S. A., Fraser, P. J., Butler, J. H., Connell, P. S., Cunnold, D. M., Daniel, J. S., Derwent, R. G., Lal, S., McCulloch, A., Oram, D. E., Reeves, C. E., Sanhueza, E., Steele, L. P., Velders, G. J. M., Weiss, R. F., and Zander, R. J.: Controlled substances and other source gases, Chapter 1 in *Scientific Assessment of Ozone Depletion: 2002*, Global Ozone Research and 500 Monitoring Project-Report No. 47, World Meteorological Organization, Geneva, Switzerland, 2003.
- Montzka, S. A., Reimann, S., Engel, A., Krüger, K., O'Doherty, S., Sturges, W. T., Blake, D., Dorf, M., Fraser, P., Froidevaux, L., Jucks, K., Kreher, K., Kurylo, M. J., Mellouki, A., Miller, J., Nielsen, O.-J., Orkin, V. L., Prinn, R. G., Rhew, R., Santee, M. L., Stohl, A., and Verdonik, D.: Ozone-Depleting Substances (ODSs) and Related Chemicals, Chapter 1, in: *Scientific Assessment of Ozone Depletion: 2010*, World Meteorological Organization, Geneva, Switzerland, 2011.
- 505 O'Doherty, S., Simmonds, P. G., Cunnold, D. M., Wang, H. J., Sturrock, G. A., Fraser, P. J., Ryall, D., Derwent, R. G., Weiss, R. F., Salameh, P., Miller, B. R. and Prinn, R. G.: In situ chloroform measurements at Advanced Global Atmospheric Gases Experiment atmospheric research stations from 1994 to 1998, *J. Geophys. Res. Atmos.*, doi:10.1029/2000JD900792, 2001.
- Palmer, P. I., Jacob, D. J., Mickley, L. J., Blake, D. R., Sachse, G. W., Fuelberg, H. E. and Kiley, C. M.: Eastern Asian emissions of anthropogenic halocarbons deduced from aircraft concentration data, *J. Geophys. Res. Atmos.*, 510 doi:10.1029/2003jd003591, 2003.



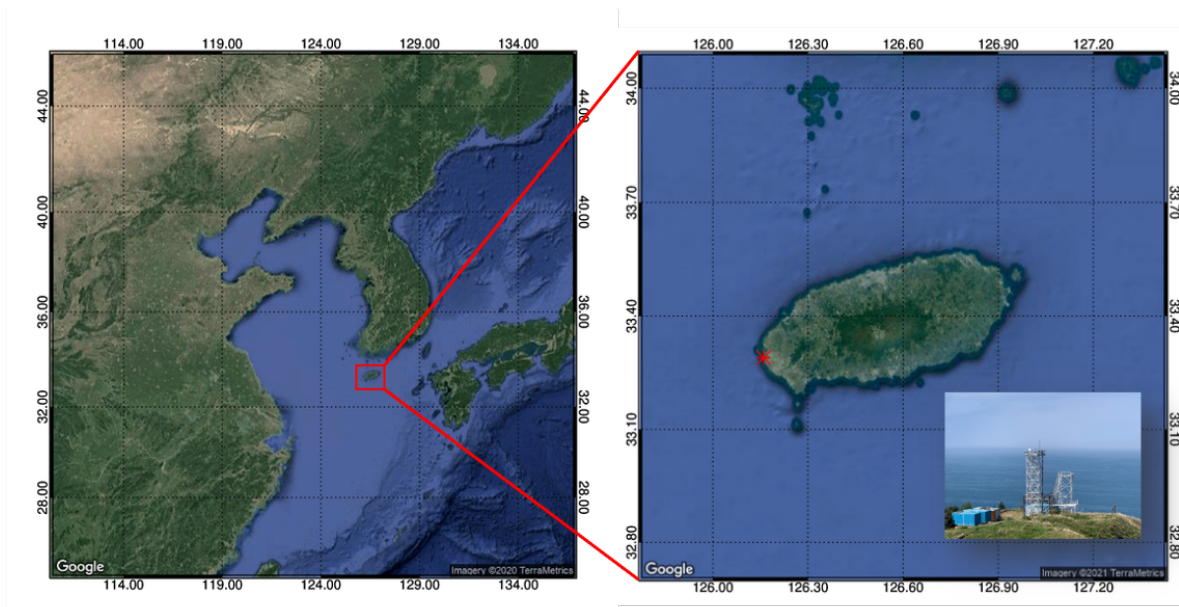
- Park, S., Li, S., Mühle, J., O'Doherty, S., Weiss, R., Fang, X., Reimann, S. and Prinn, R.: Toward resolving the mysterious budget discrepancy of ozone-depleting CCl₄: An analysis of top-down emissions from China, *Atmos. Chem. Phys.*, doi:10.5194/acp-2018-220, 2018.
- 515 Park, S., Western, L. M., Saito, T., Redington, A. L., Henne, S., Fang, X., Prinn, R. G., Manning, A. J., Montzka, S. A., Fraser, P. J., Ganesan, A. L., Harth, C. M., Kim, J., Krummel, P. B., Liang, Q., Mühle, J., O'Doherty, S., Park, H., Park, M.-K., Reimann, S., Salameh, P. K., Weiss, R. F. and Rigby, M.: A decline in emissions of CFC-11 and related chemicals from eastern China, *Nature*, doi:10.1038/s41586-021-03277-w, 2021.
- Pisso, I., Sollum, E., Grythe, H., Kristiansen, N. I., Cassiani, M., Eckhardt, S., Arnold, D., Morton, D., Thompson, R. L., Groot Zwaafink, C. D., Evangeliou, N., Sodemann, H., Haimberger, L., Henne, S., Brunner, D., Burkhardt, J. F., Fouilloux, A., 520 Brioude, J., Philipp, A., Seibert, P. and Stohl, A.: The Lagrangian particle dispersion model FLEXPART version 10.4, *Geosci. Model Dev.*, doi:10.5194/gmd-12-4955-2019, 2019.
- Porter, I. and Fraser, P.: Progress and remaining challenges with the phase-out of methyl bromide under the Montreal Protocol, *Acta Hort.*, doi:10.17660/ActaHortic.2020.1270.31, 2020.
- Press, W. H., Teukolsky, S. A., Vetterling, W. T., and Flannery, B. P.: *Numerical Recipes in C++*, 3rd Edn., Cambridge 525 University Press, Cambridge, New York, 2007.
- Prinn, R. G., Huang, J., Weiss, R. F., Cunnold, D. M., Fraser, P. J., Simmonds, P. G., McCulloch, A., Harth, C., Reimann, S., Salameh, P., O'Doherty, S., Wang, R. H. J., Porter, L. W., Miller, B. R. and Krummel, P. B.: Evidence for variability of atmospheric hydroxyl radicals over the past quarter century, *Geophys. Res. Lett.*, doi:10.1029/2004GL022228, 2005.
- Prinn, R. G., R. F. Weiss, T. Arnold, J. Arduini, L. DeWitt, P. J. Fraser, A. Ganesan, C. Harth, O. Hermansen, J. Kim, P. B. 530 Krummel, Z. M. Loh, C. R. Lunder, M. Maione, A. J. Manning, B. R. Miller, B. Mitrevski, J. Muhle, S. O'Doherty, S. Park, S. Reimann, M. Rigby, T. Saito, P. K. Salameh, R. Schmidt, P. G. Simmonds, L. P. Steele, M. K. Vollmer, R. H. Wang, B. Yao, Y. Yokouchi, D. Young and L. Zhou, History of chemically and radiatively important atmospheric gases from the Advanced Global Atmospheric Gases Experiment (AGAGE), *Earth Syst. Sci. Data*, 10, 985-1018, 2018, <https://doi.org/10.5194/essd-10-985-2018>.
- 535 Reimann, S., Schaub, D., Stemmler, K., Folini, D., Hill, M., Hofer, P., Buchmann, B., Simmonds, P. G., Grealley, B. R. and O'Doherty, S.: Halogenated greenhouse gases at the Swiss High Alpine Site of Jungfraujoch (3580 m asl): Continuous measurements and their use for regional European source allocation, *J. Geophys. Res. Atmos.*, doi:10.1029/2003jd003923, 2004.
- Rhew, R. C., Miller, B. R., Vollmer, M. K. and Weiss, R. F.: Shrubland fluxes of methyl bromide and methyl chloride, *J. 540 Geophys. Res. Atmos.*, doi:10.1029/2001JD000413, 2001.
- Rigby, M., Prinn, R. G., O'Doherty, S., Montzka, S. A., McCulloch, A., Harth, C. M., Mühle, J., Salameh, P. K., Weiss, R. F., Young, D., Simmonds, P. G., Hall, B. D., Dutton, G. S., Nance, D., Mondeel, D. J., Elkins, J. W., Krummel, P. B., Steele, L. P. and Fraser, P. J.: Re-evaluation of the lifetimes of the major CFCs and CH₃CCl₃ using atmospheric trends, *Atmos. Chem. Phys.*, doi:10.5194/acp-13-2691-2013, 2013.



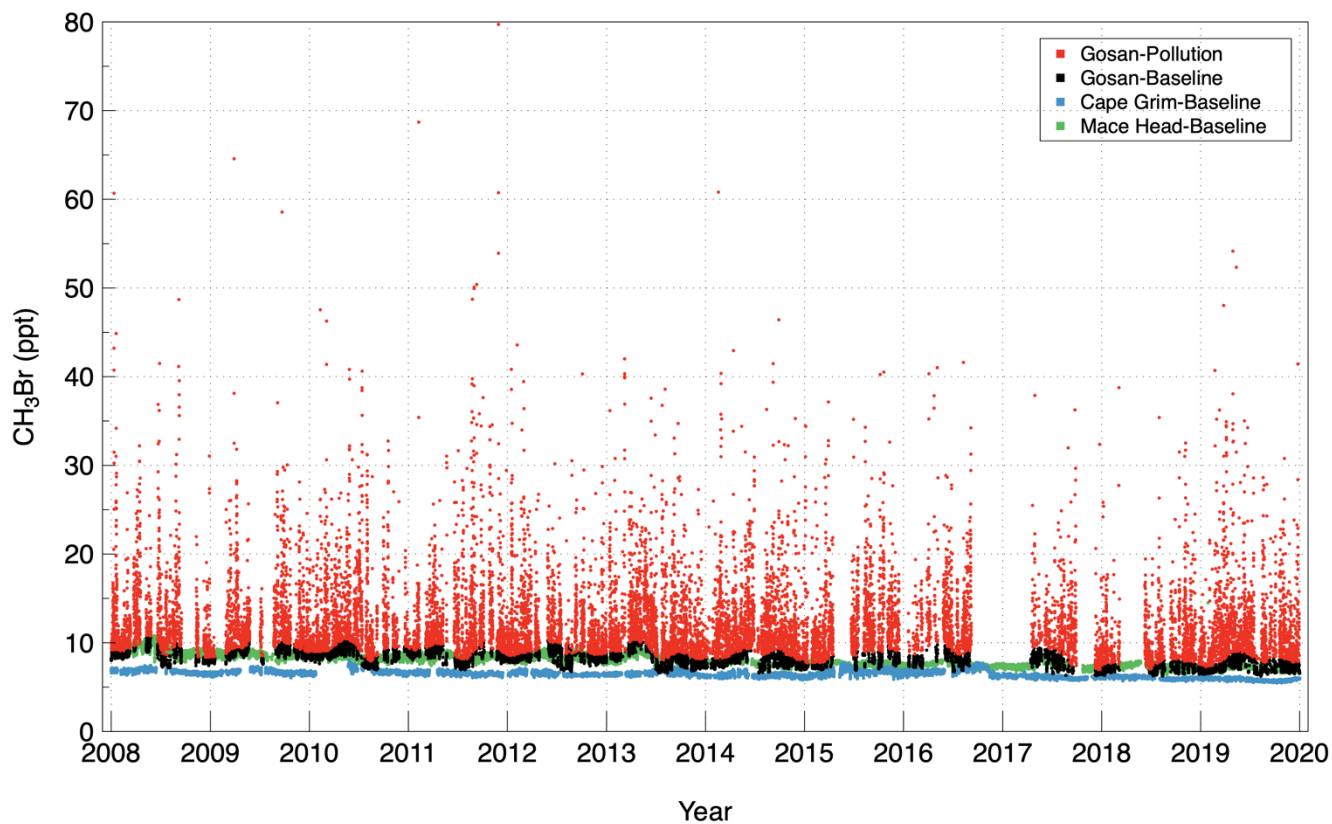
- 545 Rigby, M., Park, S., Saito, T., Western, L. M., Redington, A. L., Fang, X., Henne, S., Manning, A. J., Prinn, R. G., Dutton, G. S., Fraser, P. J., Ganesan, A. L., Hall, B. D., Harth, C. M., Kim, J., Kim, K. R., Krummel, P. B., Lee, T., Li, S., Liang, Q., Lunt, M. F., Montzka, S. A., Mühle, J., O'Doherty, S., Park, M. K., Reimann, S., Salameh, P. K., Simmonds, P., Tunnicliffe, R. L., Weiss, R. F., Yokouchi, Y. and Young, D.: Increase in CFC-11 emissions from eastern China based on atmospheric observations, *Nature*, doi:10.1038/s41586-019-1193-4, 2019.
- 550 Roberts, T., Williams, I. and Preston, J.: The Southampton system: a new universal standard approach for port-city classification, *Marit. Policy Manag.*, doi:10.1080/03088839.2020.1802785, 2020.
- Simmonds, P. G., Derwent, R. G., Manning, A. J., Fraser, P. J., Krummel, P. B., O'Doherty, S., Prinn, R. G., Cunnold, D. M., Miller, B. R., Wang, H. J., Ryall, D. B., Porter, L. W., Weiss, R. F. and Salameh, P. K.: AGAGE observations of methyl bromide and methyl chloride at Mace Head, Ireland, and Cape Grim, Tasmania, 1998-2001, *J. Atmos. Chem.*, doi:10.1023/B:JOCH.0000021136.52340.9c, 2004.
- Stohl, A.: Trajectory statistics - A new method to establish source-receptor relationships of air pollutants and its application to the transport of particulate sulfate in Europe, *Atmos. Environ.*, doi:10.1016/1352-2310(95)00314-2, 1996.
- Stohl, A., Forster, C., Frank, A., Seibert, P. and Wotawa, G.: Technical note: The Lagrangian particle dispersion model FLEXPART version 6.2, *Atmos. Chem. Phys.*, doi:10.5194/acp-5-2461-2005, 2005.
- 560 Thornton, B. F., Horst, A., Carrizo, D. and Holmstrand, H.: Methyl chloride and methyl bromide emissions from baking: An unrecognized anthropogenic source, *Sci. Total Environ.*, doi:10.1016/j.scitotenv.2016.01.213, 2016.
- TEAP (Technology and Economic Assessment Panel). Report of the Technology and Economic Assessment Panel (Volume 1). United Nations Environment Program, Nairobi, Kenya, 2020.
- Vaughn, T. L., Bell, C. S., Pickering, C. K., Schwietzke, S., Heath, G. A., Pétron, G., Zimmerle, D. J., Schnell, R. C. and Nummedal, D.: Temporal variability largely explains top-down/bottom-up difference in methane emission estimates from a natural gas production region, *Proc. Natl. Acad. Sci. U. S. A.*, doi:10.1073/pnas.1805687115, 2018.
- Vollmer, M. K., Reimann, S., Folini, D., Porter, L. W. and Steele, L. P.: First appearance and rapid growth of anthropogenic HFC-245fa (CHF₂CH₂CF₃) in the atmosphere, *Geophys. Res. Lett.*, doi:10.1029/2006GL026763, 2006.
- Vollmer, M. K., Zhou, L. X., Grealley, B. R., Henne, S., Yao, B., Reimann, S., Stordal, F., Cunnold, D. M., Zhang, X. C., Maione, M., Zhang, F., Huang, J. and Simmonds, P. G.: Emissions of ozone-depleting halocarbons from China, *Geophys. Res. Lett.*, doi:10.1029/2009GL038659, 2009.
- 570 Wallace, H. W., Jobson, B. T., Erickson, M. H., McCoskey, J. K., VanReken, T. M., Lamb, B. K., Vaughan, J. K., Hardy, R. J., Cole, J. L., Strachan, S. M. and Zhang, W.: Comparison of wintertime CO to NO_x ratios to MOVES and MOBILE6.2 on-road emissions inventories, *Atmos. Environ.*, doi:10.1016/j.atmosenv.2012.08.062, 2012.
- Wang, C., Shao, M., Huang, D., Lu, S., Zeng, L., Hu, M. and Zhang, Q.: Estimating halocarbon emissions using measured ratio relative to tracers in China, *Atmos. Environ.*, doi:10.1016/j.atmosenv.2014.03.025, 2014.



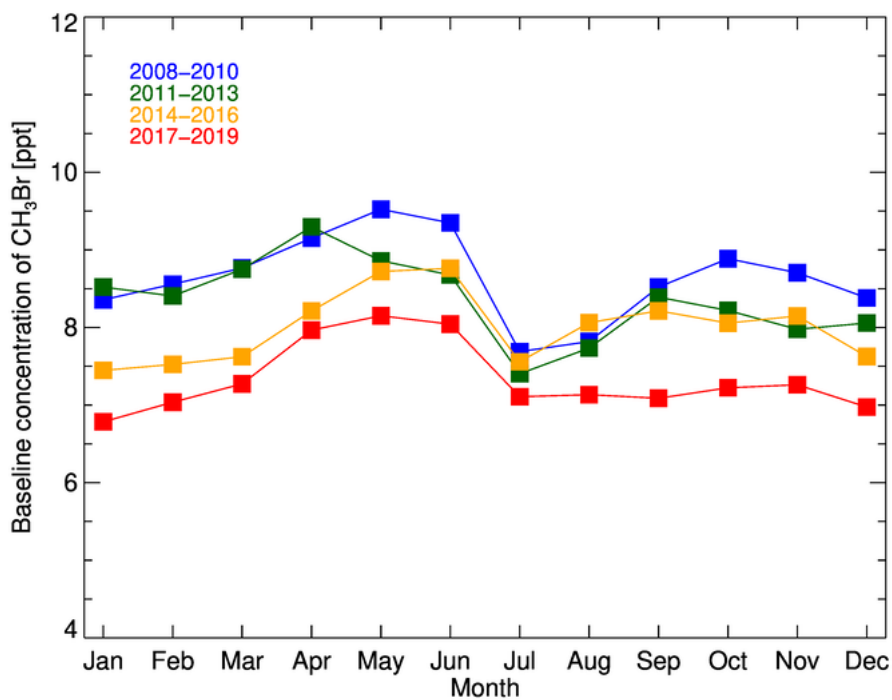
- Weinberg, I., Bahlmann, E., Eckhardt, T., Michaelis, W. and Seifert, R.: A halocarbon survey from a seagrass dominated subtropical lagoon, Ria Formosa (Portugal): Flux pattern and isotopic composition, *Biogeosciences*, doi:10.5194/bg-12-1697-2015, 2015.
- 580 Weiss, R. F. and Prinn, R. G.: Quantifying greenhouse-gas emissions from atmospheric measurements: A critical reality check for climate legislation, *Philos. Trans. R. Soc. A Math. Phys. Eng. Sci.*, doi:10.1098/rsta.2011.0006, 2011.
- Wu, C. and Zhen Yu, J.: Evaluation of linear regression techniques for atmospheric applications: The importance of appropriate weighting, *Atmos. Meas. Tech.*, doi:10.5194/amt-11-1233-2018, 2018.
- Xinyi, E., Subramanyam, B. and Li, B.: Responses of phosphine susceptible and resistant strains of five stored-product insect species to chlorine dioxide, *J. Stored Prod. Res.*, doi:10.1016/j.jspr.2017.03.002, 2017.
- 585 Yokouchi, Y., Toom-Saunry, D., Yazawa, K., Inagaki, T. and Tamaru, T.: Recent decline of methyl bromide in the troposphere, *Atmos. Environ.*, doi:10.1016/S1352-2310(02)00650-7, 2002.
- Yokouchi, Y., Taguchi, S., Saito, T., Tohjima, Y., Tanimoto, H. and Mukai, H.: High frequency measurements of HFCs at a remote site in east Asia and their implications for Chinese emissions, *Geophys. Res. Lett.*, doi:10.1029/2006GL026403, 2006.
- 590 Yvon, S. A. and Butler, J. H.: An improved estimate of the oceanic lifetime of atmospheric CH₃Br, *Geophys. Res. Lett.*, doi:10.1029/95GL03022, 1996.
- Zhang, T., De Jong, M. C., Wooster, M. J., Xu, W. and Wang, L.: Trends in eastern China agricultural fire emissions derived from a combination of geostationary (Himawari) and polar (VIIRS) orbiter fire radiative power products, *Atmos. Chem. Phys.*, doi:10.5194/acp-20-10687-2020, 2020.
- 595 Zhao, H., Zhang, X., Zhang, S., Chen, W., Tong, D. Q. and Xiu, A.: Effects of agricultural biomass burning on regional haze in China: A review, *Atmosphere (Basel)*, doi:10.3390/atmos8050088, 2017.



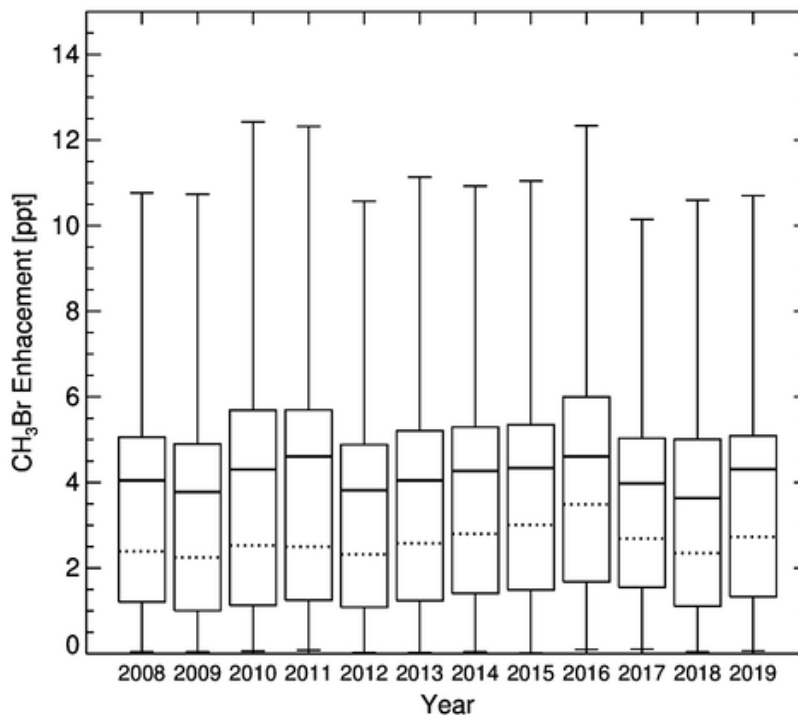
600 **Figure 1: Gosan station (33.3° N, 126.9° E, 72 m a.s.l.) on Jeju island, Korea (red asterisk). Air samples are taken at 17 m (~100 m a.s.l.) from a tower next to the coastal cliff. (Map data: © Google Earth)**



605 **Figure 2: Concentrations of CH₃Br in the atmosphere at Gosan for the period 2008–2019. The baseline data (black) are selected using a statistical method (O’Doherty et al., 2001); the polluted data (red) are elevated above the baseline data. The baseline data from Mace Head, Ireland (green) and Cape Grim, Australia (blue) over the same period are shown as mid-latitude references for the Northern and Southern Hemisphere, respectively.**



610 **Figure 3: Monthly mean CH₃Br baseline concentrations at Gosan for 2008–2019. Each color represents the average of the 3-year interval for the period. Note that there are data missing for several months in 2016, 2017, and 2018, mainly due to typhoon damage to Gosan station.**



615 **Figure 4: Box-whisker plot of annual enhancements of CH₃Br at Gosan for 2008–2019. The box encloses the interquartile range (IQR) defined at 25–75 percentiles, and whiskers represent maximum (top) and minimum (bottom) enhancements. The solid and dot lines in the boxes represent the mean and median value of the data, respectively.**

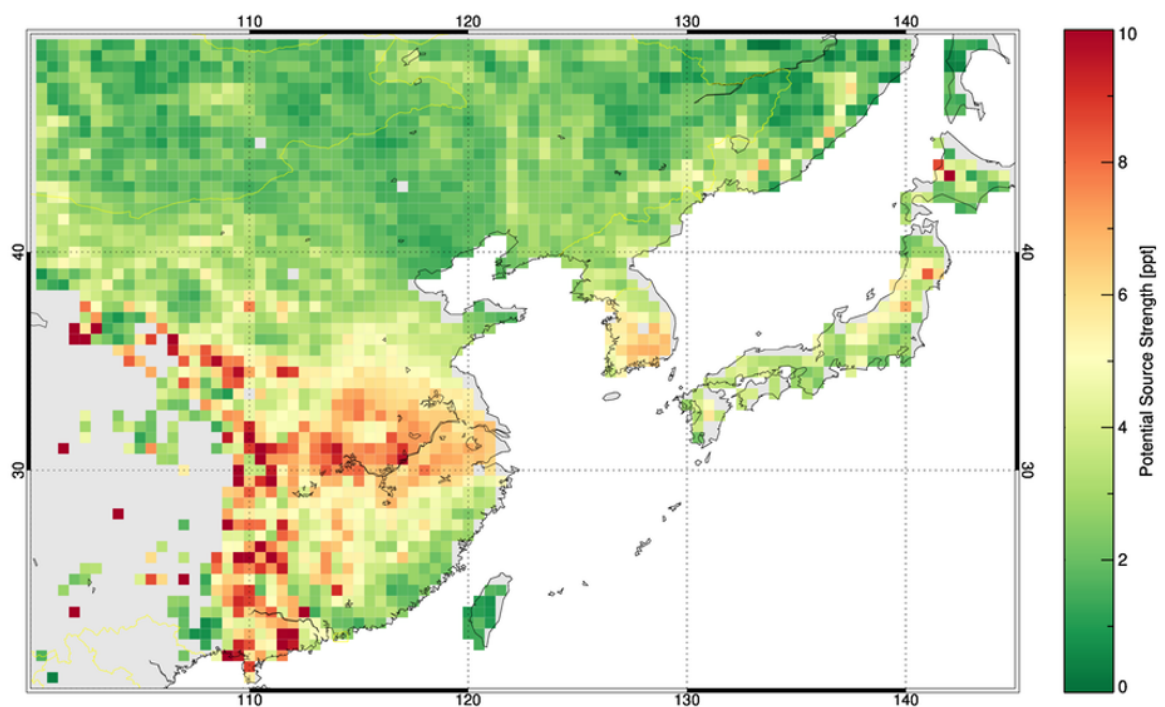


Figure 5: Potential source regions for CH_3Br emissions derived by back-trajectory analyses of enhanced CH_3Br concentrations measured at Gosan station from 2008 to 2019.

620

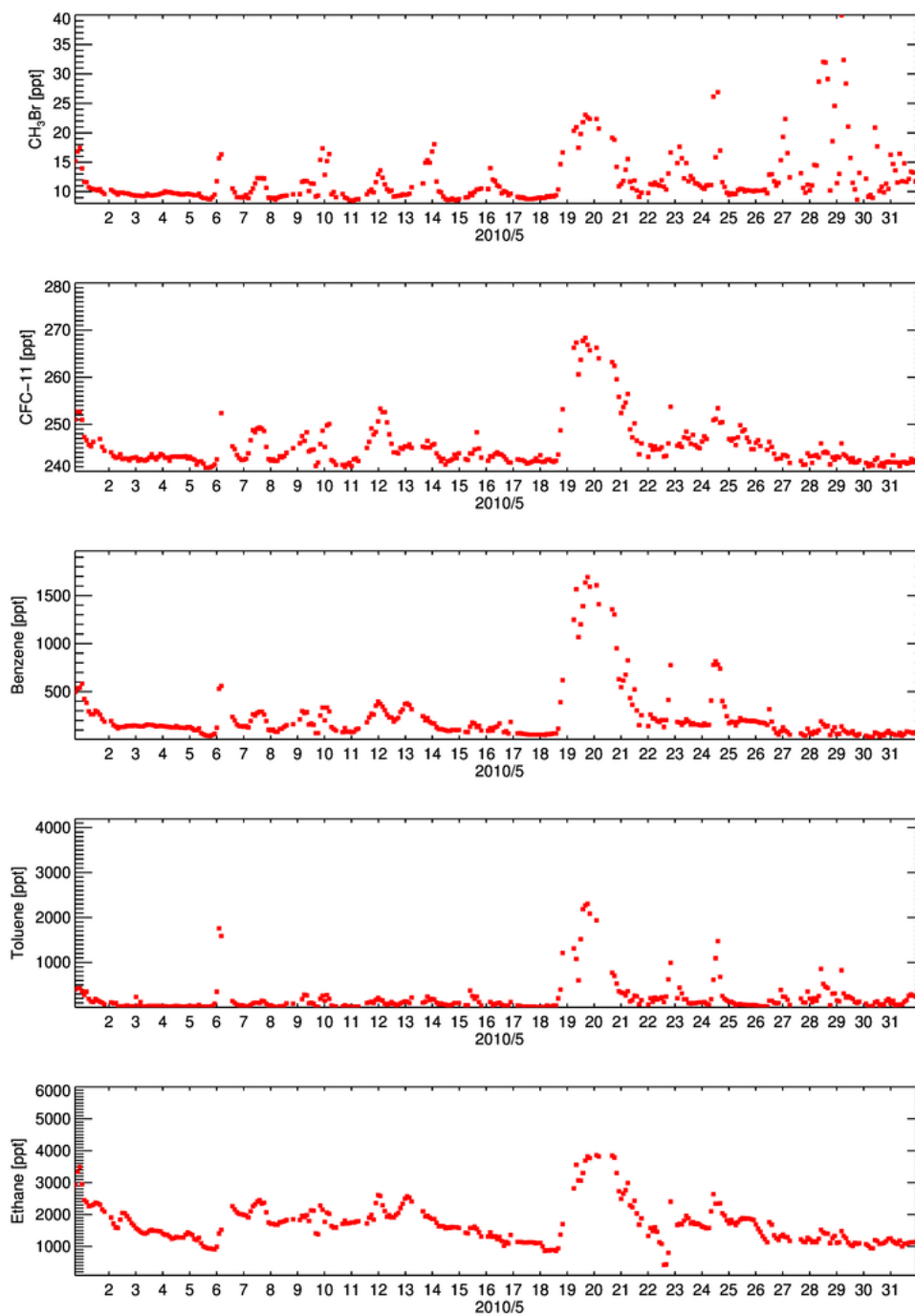
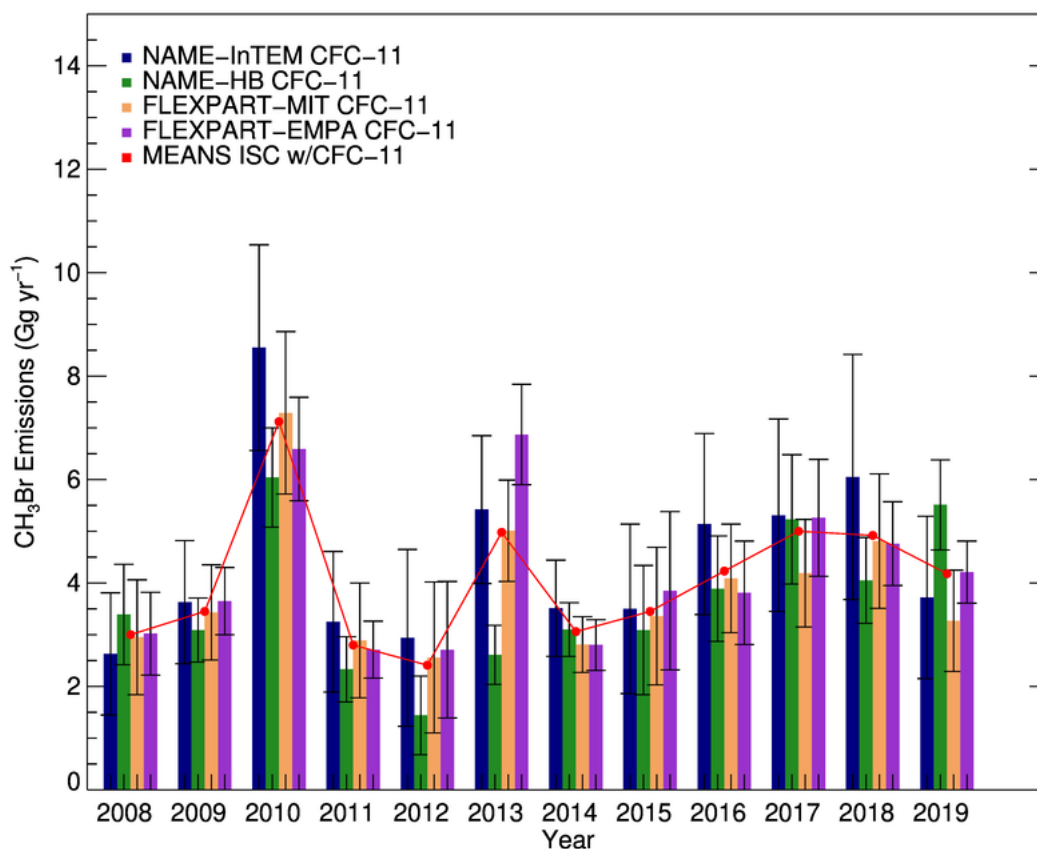
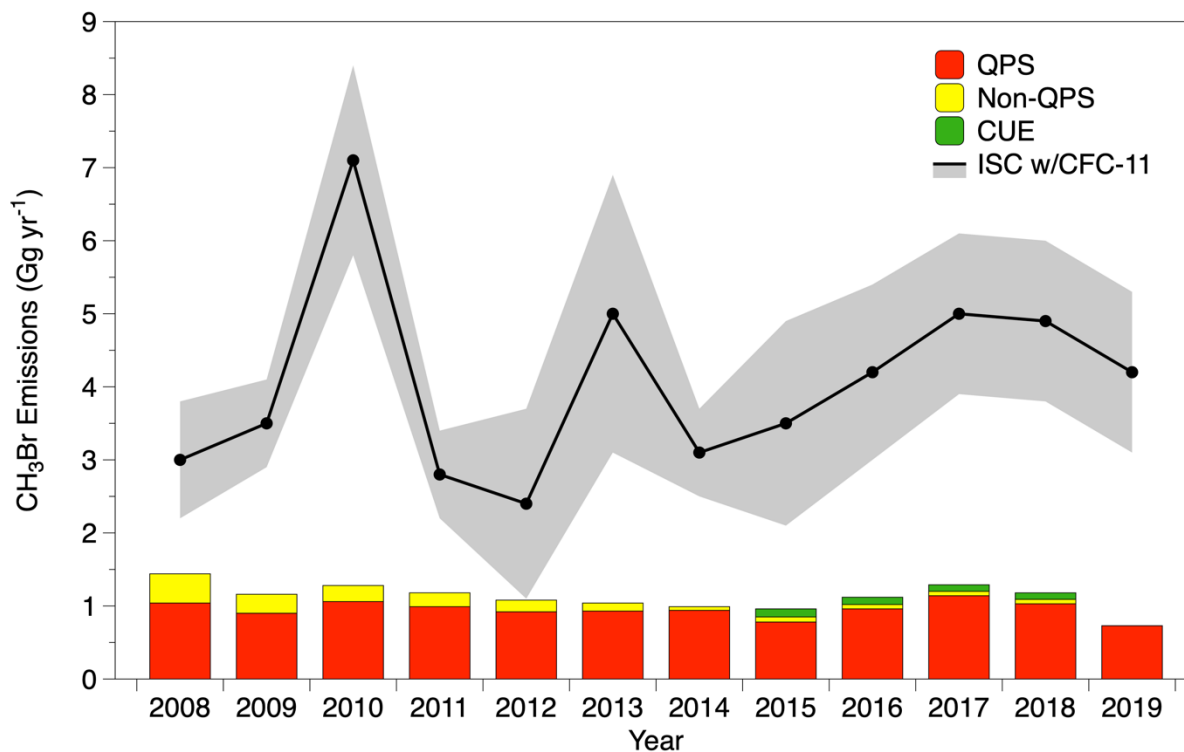


Figure 6: Observed concentrations of CH₃Br, CFC-11, benzene, toluene, and ethane at Gosan during May 2010; note the highly correlated pollution events between CH₃Br and CFC-11, also the concentrations of VOCs (benzene, toluene, and ethane), which are likely related to the biomass burning and general anthropogenic combustion processes increased simultaneously.



630 **Figure 7:** CH₃Br emission estimates derived for eastern China by ISC from the observation data of CH₃Br and CFC-11 at Gosan during 2008–2019. CFC-11 emissions were taken from Park et al. (2021) and are estimated using four-independent inverse model frameworks (NAME-HB, NAME-InTEM, FLEXPART-MIT and FLEXPART-Empa). The bar plot of each color denotes the emission of CH₃Br with 1 sigma uncertainty derived from each inversion of CFC-11, and the average of the four different inversions is shown in red.



635 **Figure 8: Top-down emissions of CH₃Br for eastern China estimated by ISC using CFC-11 as the reference tracer (Figure 7). The bottom-up emissions of CH₃Br for China are based on the reported consumption data to UNEP for quarantine/pre-shipment (QPS), non-QPS and critical use exemption (CUE) categories.**



Table 1: Annual means and standard deviations of CH₃Br baseline data and observed pollution signals at Gosan 2008 to 2019.

Year	Baseline		Pollution	
	CH ₃ Br (ppt)	Number of data	CH ₃ Br (ppt)	Number of data
2008	8.5 ± 0.8	933	13.1 ± 5.1	1402
2009	8.7 ± 0.5	955	13.0 ± 4.6	1187
2010	8.6 ± 0.8	1215	13.2 ± 4.9	1485
2011	8.4 ± 0.7	938	13.4 ± 6.2	1395
2012	8.4 ± 0.6	1069	12.5 ± 4.3	1360
2013	7.9 ± 0.9	1065	12.7 ± 4.4	1831
2014	7.9 ± 0.6	967	12.5 ± 4.7	1715
2015	7.8 ± 0.7	497	12.6 ± 4.6	1263
2016	8.0 ± 0.7	445	13.4 ± 4.4	688
2017	7.8 ± 0.9	425	11.7 ± 4.0	582
2018	7.0 ± 0.4	691	10.9 ± 3.9	899
2019	7.4 ± 0.6	1105	12.1 ± 5.0	1655



Table 2: Bottom-up and top-down emissions of CH₃Br from 2008 to 2019 as presented in Figure 8. The bottom-up emissions are the sum of QPS, non-QPS and CUE consumption as reported to UNEP for all of China (data available at Ozone Secretariat website, <http://ozone.unep.org>). The top-down emissions were derived for eastern China by ISC method with CFC-11 as the reference tracer.

Year	UNEP reported (Gg yr ⁻¹)			Total	ISC (CFC-11 ref.) (Gg yr ⁻¹)
	QPS	Non-QPS	CUE		
2008	1.04	0.40	-	1.44	3.0 ± 0.8
2009	0.90	0.26	-	1.16	3.5 ± 0.6
2010	1.06	0.22	-	1.28	7.1 ± 1.3
2011	0.99	0.19	-	1.18	2.8 ± 0.6
2012	0.92	0.16	-	1.08	2.4 ± 1.3
2013	0.93	0.11	-	1.04	5.0 ± 1.9
2014	0.94	0.05	-	0.99	3.1 ± 0.6
2015	0.78	0.07	0.11	0.96	3.5 ± 1.4
2016	0.96	0.06	0.10	1.12	4.2 ± 1.2
2017	1.14	0.06	0.09	1.29	5.0 ± 1.1
2018	1.03	0.06	0.09	1.18	4.9 ± 1.1
2019	0.73	0	-	0.73	4.2 ± 1.1

QPS: quarantine/pre-shipment, CUE: critical use exemptions, UNEP: United Nations Environment Programme